ISSN 0965-545X, Polymer Science, Ser. A, 2015, Vol. 57, No. 6, pp. 910–923. © Pleiades Publishing, Ltd., 2015.
Original Russian Text © S.O. Ilyin, 2015, published in Vysokomolekulyarnye Soedineniya. Ser. A, 2015, Vol. 57, No. 6, pp. 568–581.

Non-linearity in Rheological Properties of Polymers and Composites under Large Amplitude Oscillatory Shear

S. O. Ilyin

Topchiev Institute of Petrochemical Synthesis, Russian Academy of Sciences, Leninskii pr. 29, Moscow, 119991 Russia
e-mail: s.o.ilyin@gmail.com

Received April 30, 2015;
Final Manuscript Received June 29, 2015

Abstract—Various approaches to the calculation of the components of the dynamic modulus measured at large amplitude oscillatory shear are compared. The method of Fourier analysis using Chebyshev polynomials, the determination of moduli via the differentiation of stress at the points of zero and maximum deformations, and the integration of the Lissajous figures are considered. A comparative analysis of material-nonlinearity measures obtained through various methods is performed. The measures of viscous and elastic nonlinearities, the mechanical-loss tangent of the material, and the power of its response are compared. The investigation is conducted for model samples of polyisobutylene in viscous-flow and high-elastic relaxation states and polyisoprene filled with nanoparticles of silicon oxide.

DOI: 10.1134/S0965545X15060103

INTRODUCTION

One of the conventional methods for the investigation of rheological properties of materials is the method of small amplitude oscillatory shear [1]. During its application, the studied sample is deformed with frequency ω according to a harmonic law with a given low strain amplitude: $\gamma(t) = \gamma_0\sin(\omega t)$. "Low amplitude" is taken to mean such a value of deformation at which stresses arising in the material are directly proportional to it. In this case, the time dependence of stresses is likewise harmonic: $\sigma(t) = \sigma_0\sin(\omega t + \delta)$. Mechanical-loss angle δ characterizes the part of energy that the material loses in a deformation cycle and is equal to 0° for an absolutely elastic body and 90° for an absolutely viscous liquid. The dynamic complex modulus can be written in the form

$$G^* = \frac{\sigma(t)}{\gamma(t)} = G' + iG'' = \frac{\sigma_0}{\gamma_0}\cos\delta + i\frac{\sigma_0}{\gamma_0}\sin\delta \qquad (1)$$

The situation changes fundamentally during a periodic deformation of the material with a large amplitude when the material response (stress) is no longer a regular harmonic.

A convenient method for visualization of the results is abandonment of the application of time as an argument and construction of the Lissajous figures, i.e., the dependence of stress on deformation. For linear viscoelastic behavior, these figures are ellipses, and, in the case of a nonlinear response of the sample, they transform into figures of variable shapes [2, 3].

The interest in the analysis of nonlinear viscoelasticity of materials via the method of large amplitude oscillatory shear appeared in the 1970s [4]. In recent years, a number of methods for analysis of the nonharmonic response of samples have been suggested (see, e.g., review [5]). A goal of analysis of the nonlinear response of samples may be determination of their objective rheological characteristics in relation to the structure [6–11], elucidation of the parameters of the model that fits their behavior [12–15], or observation over physical processes during their deformation [12, 16–24]. Some studies have been devoted to the choice of the deformation mode [25, 26], the measurement geometry [27, 28], and application of the microrheology method [29].

To estimate the nonlinearity of materials, their objective rheological characteristics derived from tests in the nonlinear region of mechanical behavior are used. The most popular approach to establishing nonlinear characteristics is the following sequence of actions. First is the transformation of a nonlinear response into a Fourier series [30] and the expansion of stress into components [31]:

$$\sigma(t) = \sigma'(t) + \sigma''(t) = \gamma_0\left(\sum_{n,\text{odd}} G'(\omega,\gamma_0)\sin(n\omega t) + \sum_{n,\text{odd}} G''(\omega,\gamma_0)\cos(n\omega t)\right) \qquad (2)$$

Only odd higher harmonics are considered, while it is assumed that even ones result from flow non-homogeneity [32].

Then, the response is approximated with the use of Chebyshev polynomials of the first kind so that elastic

and viscous responses can be presented in the following form [33]:

$$\sigma'\left(\frac{\gamma}{\gamma_0}\right) = \gamma_0 \sum_{n,\text{odd}} e_n(\omega,\gamma_0) T_n\left(\frac{\gamma}{\gamma_0}\right)$$
$$\text{and} \quad \sigma''\left(\frac{\dot\gamma}{\dot\gamma_0}\right) = \dot\gamma_0 \sum_{n,\text{odd}} \nu_n(\omega,\gamma_0) T_n\left(\frac{\dot\gamma}{\dot\gamma_0}\right), \tag{3}$$

where e_n and ν_n are the elastic and viscous Chebyshev coefficients and T_n is the Chebyshev polynomial of the nth order.

As a final result, these manipulations make it possible to calculate the components of the dynamic modulus at large (G_L) and minimal deformations (G_M):

$$G'_L = \sum_{n,\text{odd}} e_n, \quad G''_L = \omega \sum_{n,\text{odd}} \nu_n,$$
$$G'_M = \sum_{n,\text{odd}} (-1)^{\frac{n-1}{2}} n e_n, \quad G''_M = \omega \sum_{n,\text{odd}} (-1)^{\frac{n-1}{2}} n \nu_n. \tag{4}$$

From the physical point of view, the component at a large deformation includes the linear and nonlinear part of the dynamic modulus of the material. For example, it can be written in the form of a simple model:

$$G_L = G_0 + G_\beta(\gamma/\gamma^*), \tag{5}$$

where γ^* is deformation that causes a nonlinear response. The component at minimal deformation, G_M, is only a linear part, i.e., G_0.

From the mathematical point of view, the elastic component at a large deformation is the derivative of stress at the point where deformation is maximal, and the component at the minimal deformation is the derivative at the point where deformation takes a zero value. For the viscous component, the definition is analogous with exclusion of the fact that the derivative is taken with respect to the rate of deformation, rather than the deformation itself:

$$G'_M = \left.\frac{d\sigma}{d\gamma}\right|_{\gamma=0}, \quad G'_L = \left.\frac{\sigma}{\gamma}\right|_{\gamma=\gamma_0},$$
$$G''_M = \omega\left.\frac{d\sigma}{d\dot\gamma}\right|_{\dot\gamma=0}, \quad G''_L = \omega\left.\frac{\sigma}{\dot\gamma}\right|_{\dot\gamma=\dot\gamma_0}. \tag{6}$$

Finally, for classification of materials, it was suggested to use the measures of elastic nonlinearity S and viscous nonlinearity T, defined by the relationships

$$S = \frac{G'_L - G'_M}{G'_L} \quad \text{and} \quad T = \frac{G''_L - G''_M}{G''_L}. \tag{7}$$

Positive measures indicate the elastic or viscous hardening of a material, whereas negative values indicate the corresponding softening.

An alternative to the Fourier transformation of the material response is the integral method of definition of the components of the dynamic modulus at large and small deformations, which is based on the application of the Lissajous figures [34, 35]. The main point is that the loss modulus at a large deformation is proportional to the area of the Lissajous figure built in stress–deformation coordinates, and the elasticity modulus at a high deformation is proportional to the area of the figure in coordinates of the derivative of stress with respect to the phase angle and deformation:

$$G'_L = \frac{E}{\pi\gamma_0^2} \quad \text{and} \quad G''_L = \frac{A}{\pi\gamma_0^2}. \tag{8}$$

Here, E is the area of the figure in $d\sigma/d(\omega t)$–γ coordinates, while A is the area of the figure in the conventional σ–γ coordinates.

The elasticity and loss moduli can be calculated for the moment time where the deformation reaches the maximal value. A difference of such differential or instantaneous modulus G_R from the modulus at a large deformation consists in the fact that the former is some momentary value at the point of maximal deformation, while the latter is the combined averaged modulus that characterizes the material during its deformation from zero to the maximal magnitude.

To find the instantaneous modulus, it is possible to use two Lissajous figures obtained at close values of deformation, and the instantaneous modulus itself (for example, elasticity modulus) can be written as

$$G'_R(\gamma_0) = \lim_{\Delta\gamma\to 0} \frac{\Delta E}{\pi\Delta\gamma(2\gamma_0 - \Delta\gamma)}$$
$$\approx \frac{G'_L(\gamma_0)\times\gamma_0^2 - G'_L(\gamma_0 - \Delta\gamma)\times(\gamma_0 - \Delta\gamma)^2}{\gamma_0^2 - (\gamma_0 - \Delta\gamma)^2}, \tag{9}$$

where ΔE is the difference between the area of the Lissajous figure obtained at an amplitude of deformation of γ_0 and the area of the analogous figure, but at a lesser amplitude of deformation.

The modulus at a large deformation, the modulus at the minimal deformation, and the instantaneous modulus are interconnected [34]:

$$G_M = 2G_L - G_R. \tag{10}$$

The determination of the nonlinear components of the dynamic modulus via the integral method makes it possible to calculate the measures of elastic and viscous nonlinearity through Eq. (7). However, the Lissajous figures themselves can be additionally used to search for alternative measures of nonlinearity according to the distortion of the ellipse shapes [35]. For this purpose, the Lissajous figure must be divided into four parts along the ordinate axis and a straight line that combines the experimental points with the amplitude deformation. Then, it is necessary to subtract from the area of sectors that are responsible for the development of deformation from zero to the amplitude value the areas of opposite sectors where deformation decreases in amplitude to zero value. Referring the resulting value to the total area of the Lissajous figure gives the measure of nonlinearity:

$$S_A = \frac{E_{\gamma \ni d|\gamma|/dt>0} - E_{\gamma \ni d|\gamma|/dt<0}}{E}$$
$$\text{and} \quad T_A = \frac{A_{\gamma \ni d|\gamma|/dt>0} - A_{\gamma \ni d|\gamma|/dt<0}}{A}. \quad (11)$$

Subsequently, for convenience, let us add the following to the recording of moduli and nonlinearity measures obtained with the use of the Fourier transformations: lower index F; in the case of integration of the Lissajous figures, index I; and for nonlinearity measures obtained via the division of the Lissajous figure, index A (as in Eq. (11)).

Hence, two different approaches to the analysis of the nonlinear material response can be highlighted. They are utilized to define the components of the dynamic modulus and the measures of material nonlinearity. The first approach is based on the Fourier analysis of the material response, while the second approach is based on the integration of the dependences of stress and its derivative with respect to phase angle over deformation.

The goal of the present study is to compare the results derived via two approaches relative to the model systems. In other words, the case in point is the comparison of particular values of nonlinear storage and loss moduli as well as the measures of elastic and viscous nonlinearity. Moreover, consideration is given to other possible approaches to the analysis of the nonlinear behavior of samples for establishing the usefulness of the method of large amplitude oscillatory shear as a method that supplements conventional testing techniques.

EXPERIMENTAL

The investigation was concerned with two model systems: polyisobutylene (PIB) in the viscous-flow and high-elasticity relaxation states and *cis*-1,4-polyisoprene (PIP) filled with silicon dioxide nanoparticles. PIB with $M_w = 51 \times 10^3$ and a polydispersity index of 4.0 was supplied by BASF (trademark Oppanol B12 SFN). PIP was with $M_n = 65 \times 10^3$ and a polydispersity index of 1.4 was supplied by Royal Adhesives and Sealants (trademark Isolene 400). Silicon dioxide (Sigma Aldrich) had an average size of elementary particles of 7 nm and a specific surface of 395 m^2/g.

SiO_2 was introduced into a 30% solution of PIB in *n*-hexane under stirring on an IKA Ultra-Turrax T 18 disperser at a rotor rotation speed of 24×10^3 rotations/min. After stirring, the solvent was removed under vacuum at a temperature of 100°C. The composites were studied with filler contents of 3, 5, 7, and 9 vol %.

The rheological properties were studied on a Physica MCR 301 Anton Paar rotation rheometer with controlled shear stress and a cone–plane unit (d = 20 mm, $\alpha = 2°$). The sample testing was performed in the mode of periodic deformation according to a harmonic law with a particular given amplitude of deformation and measurement of stress as the system response.

The properties of PIB were studied at 20°C with impact frequencies of 1, 3, 10, and 30 Hz and at 150°C with a frequency of 3 Hz. The properties of PIP composites were investigated at 20°C and a frequency of 1 Hz.

RESULTS AND DISCUSSION

Polyisobutylene

The effect of the relaxation state of the polymer and the frequency of its loading on the complex of viscoelastic properties at large deformations was studied for the example of PIB. Its viscoelastic properties in the linear range of mechanical behavior, as well as the results of data translation to 20°C with the use of the principle of temperature–time superposition [36], are presented in Fig. 1. They are typical for polymers with broad molecular-mass distributions, a circumstance that is reflected in the smooth transition from one physical state to another and in the incline of the high-elasticity plateau. The experiments utilizing large deformations were performed for the example of PIB in the viscous-flow and high-elasticity states (vertical lines in Fig. 1).

During application of the method based on the Fourier transformation, the following questions arise: How much higher should the harmonics that are considered during analysis be (for example, only to seventh)? Should the even harmonics be considered? Do they have any physical meaning, or are they noise? Let us consider the evolution of harmonic magnitudes (i.e., complex moduli) with an increase in deformation amplitude (Fig. 2).

In the range of low amplitudes of strain and stress, the complex modulus manifests the second, third, and fifth harmonics that differ from zero. The appearance of higher harmonics is explained by the background vibrations, a circumstance that becomes evident only at a low torque on the rheometer drive. Indeed, the vibration distorts the input signal, so that a part of the first harmonic of deformation decreases to 97%, and the nonlinearity of the impact on the object leads to the nonlinearity of its response.

As the stress applied to the sample increases, the background noise becomes insignificant and both signals appear to be harmonic. As the amplitude increases, a decrease in the portion of the first harmonic is again substantial at a deformation exceeding 300%. The deviation from the harmonic law is likely to be observed as a result of the use of rheometers with controlled shear stress during testing of materials in the mode of controlled deformations. The maximal distortion of the input signal is reached at a deformation amplitude of ~8000%; therefore, a portion of the first harmonic becomes equal to 95%. A further

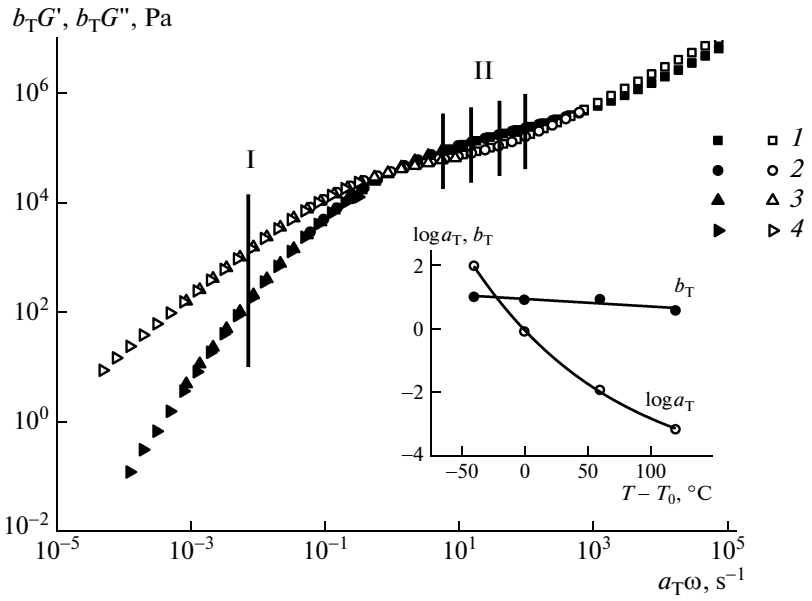

Fig. 1. (Closed circles) The linear storage and (open circles) loss moduli of PIB in the (I) viscous-flow and (II) high-elasticity states normalized to 20°C. $T = (1) -20$, (2) 20, (3) 80, and (4) 140°C. The inset shows the temperature dependences of normalization factors. The vertical lines denote the chosen temperature–time conditions for further experiments in the nonlinear region.

increase in the amplitude of the input signal leads to weak monotonic suppression of distortion. On the whole, analogous behavior is demonstrated by the second harmonic of the output signal: Its appearance coincides with the beginning of considerable distortion of the input impact and it reaches the maximal portion (1.5%) at a deformation of ~1000% and then gradually decreases. Hence, the appearance of the second harmonic of the output signal is very likely to be caused precisely by the distortion of the input signal. In any case, only the second harmonic proceeds through a maximum as the amplitude of impact increases along with the degree of distortion of the input impact.

The odd modulus harmonics increase monotonically as the amplitude of deformation grows and appear gradually: from the third to the seventh harmonic during an increase in deformation by approximately a decimal exponent. The difference in deformation between appearance of the seventh, ninth, and further harmonics is not as high. However, the higher harmonics become evident only at a deformation exceeding 10^5%, which actually corresponds to the limit of rheometer possibilities. Moreover, testing of a material with such a deformation (and rate) can lead to adhesion or cohesion breaks with loss of contact with the measuring unit or loss of continuity of the studied sample. Furthermore, the material may creep out from the measuring gap owing to the appearance of the Weissenberg effect. In other words, such high amplitudes of the impact and harmonics are not of practical interest.

From the presented data, it follows that, for the analysis using the Fourier transformation, it is possible to use only the first, third, and fifth harmonics. The seventh and ninth harmonics can additionally be taken into account because their growth during an increase in the impact amplitude is monotonic. This circumstance means that the mentioned higher harmonics reflect the changes in material properties, and, although their portion is negligible, it cannot be excluded that, in more complex systems, it can be higher. Nevertheless, consideration of the higher harmonics (or even the whole series) is not acceptable, owing to their application for some calculations in the form multiplied by its number (for example, during the definition of moduli at the minimal deformation via Eq. (4)). For further calculations, only odd harmonics up to the ninth will be considered.

Let us compare the results of the application of the known methods for the calculation of nonlinear viscoelastic characteristics to one set of the primary data (Fig. 3). The storage modulus, regardless of the used method, can be calculated up to deformations of ~10^5%. According to the data of Fig. 2, during precisely such deformations, the harmonics above the seventh become evident in the output signal. At large deformations, a broad dispersion of points and negative values of the calculated storage moduli are observed. For loss moduli, owing to their lower dependence on the deformation amplitude (high values compared to the accumulation modulus), it is possible to define their values in the whole studied range, which, nevertheless, in isolation from the simulta-

neous estimation of the material elasticity has no meaning.

The values of nonlinear moduli established via the integration of the Lissajous figures, G_I, and established via the Fourier analysis of the output signal, G_F, do not coincide. However, the difference in each modulus at a fixed value of amplitude is not high, and all nonlinear moduli are extremely close in value to the modulus calculated via the most apparent method: for the first harmonic of the output signal. Nevertheless, in the case of application of the integral method, during the definition of moduli at minimal and large deformations, a substantial difference between these values arises simultaneously with the output of material from the region of linear viscoelasticity, whereas, during application of the method of analysis of harmonics, a substantial difference between the two moduli is observed only at considerable deformations (above 1000%, Fig. 3). In addition, a pronounced deviation of the Lissajous figures from an ellipse occurs at lower values of deformation amplitudes (insets in Fig. 3). In other words, moduli G_F are not as sensitive to the input impact as G_I is in the range of not very high deformation amplitudes.

The moduli at minimal and large deformations can be calculated directly through formula (6) with the use of the mathematical definition of these values. Let us do so for the Lissajous figures demonstrated in the insets of Fig. 3 and compare the resulting values with the values obtained via the two other methods (table).

The data of the table indicate that, despite a significant deviation of the output signal from the harmonic type, all moduli, irrespective of whether they were obtained at large or minimal deformations, are close. Against the other moduli, only the modulus at the minimal deformation, $G_{M,I}$, defined by the Lissajous figures differs. In the physical meaning, the value of modulus G_M must be equivalent to the linear component of the modulus of a studied body (see Eq. (5)); i.e., it must be close in value to the modulus in the range of linear viscoelasticity. It is apparent that this is obeyed best of all precisely by moduli obtained via the integration.

On the whole, the considered methods give the same character of amplitude dependences of the components of the dynamic modulus and only insignificantly differ in value at the same amplitude of the sample deformation. Consequently, much more significant are their ratios as measures that characterize the nonlinearity of the studied object. Let us compare the measures of nonlinearity obtained via three methods. Two of them utilize the ratios of moduli at large and minimal deformations calculated in the analysis of the Lissajous figures (S_I and T_I) or in the Fourier analysis (S_F and T_F) through Eq. (7), and the third utilizes the ratio of areas of Lissajous figure sectors (S_A and T_A) through Eq. (11).

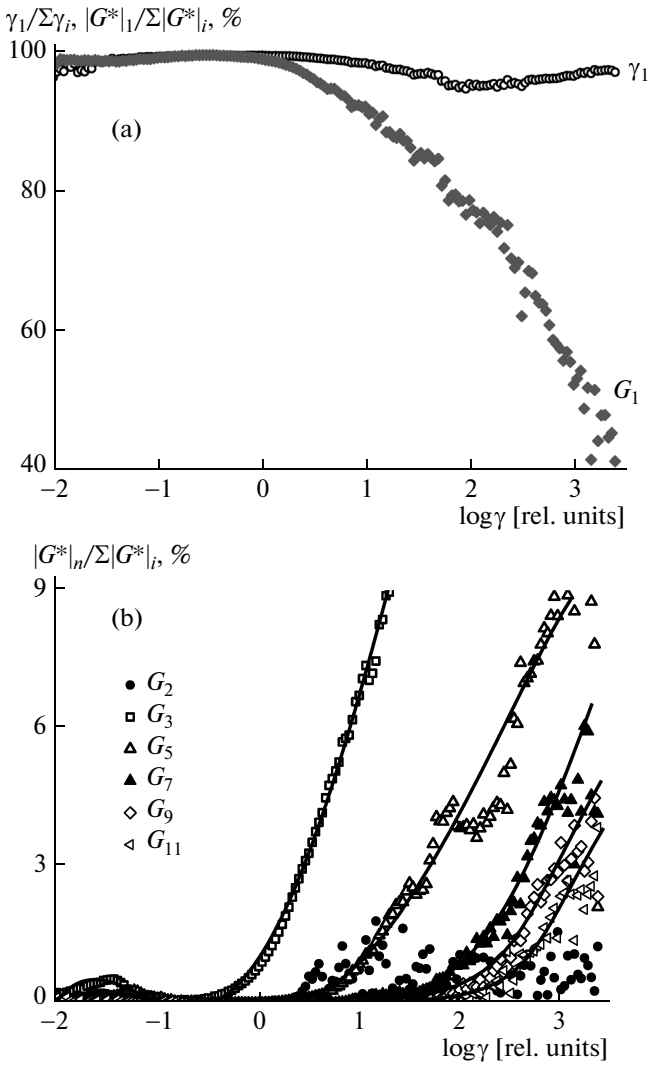

Fig. 2. (a) Portion of the first harmonics of deformation, γ_1, and complex modulus G_I and (b) the portion of the nth harmonics of the complex modulus in the deformation or the modulus in a dynamic test of PIB at 20°C and an angular frequency of 6.28 s^{-1}.

The signs of the measures of elastic nonlinearity established via different methods (Fig. 4a) in general indicate the strain softening of the polymer at large deformations and strain stiffening at very large deformations, whereas the measures of viscous nonlinearity (Fig. 4b) testify pseudoplasticity. Only numerical values of these measures and the deformation amplitude at which a transition from one model to another occurs differ.

The nonlinearity measures calculated via the Fourier analysis appear to be more sensitive to the change in amplitude of the input impact than the components of dynamic modulus defined by the same method. However, unlike the measures found via another method, measures S_F and T_F indicate weak strain stiffening at relatively small deformations and the transi-

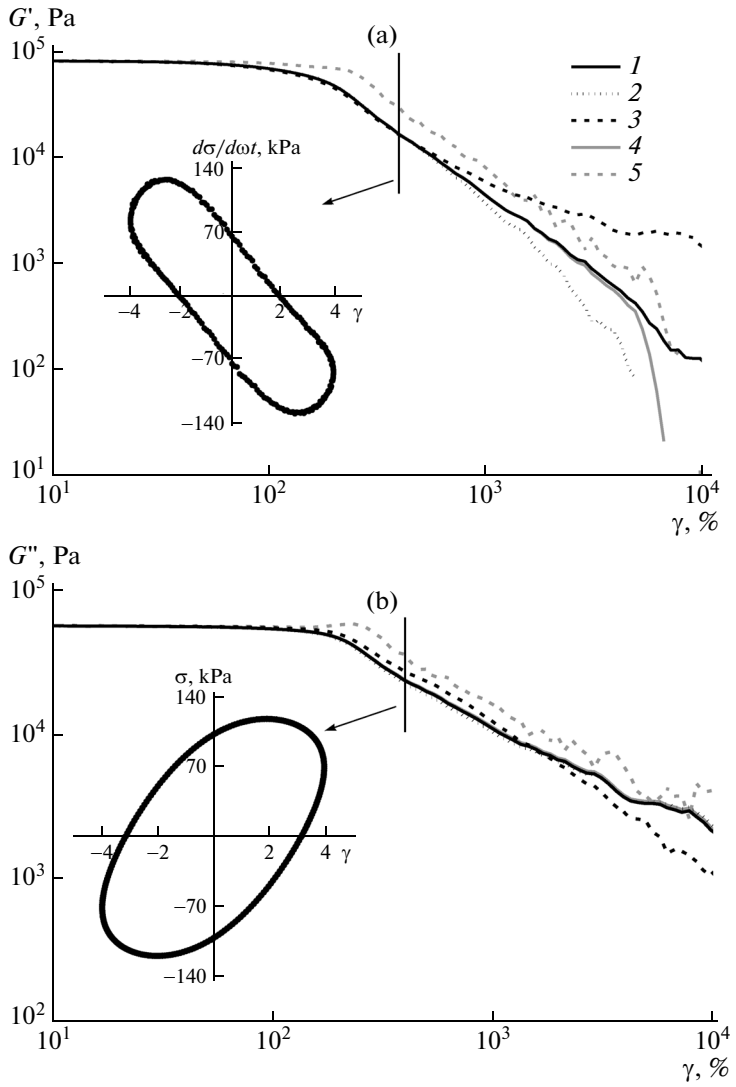

Fig. 3. Amplitude dependences of (a) storage modulus G' and (b) loss modulus G'' of PIB at 20°C and an angular frequency of 6.28 s^{-1}: (*1*) G_I, (*2*) $G_{L,F}$, (*3*) $G_{M,F}$, (*4*) $G_{L,I}$, (*5*) $G_{M,I}$. The insets show the Lissajous figures obtained at a deformation amplitude of 400%.

tion from shear thinning to shear thickening at deformations above 2000%, respectively. The latter, however, cannot be correct, because there is no increase in viscosity with the shear rate during testing of PIB.

During discussion of the results, a legitimate question is the need for the nonlinearity measures. It seems they are necessary not only for classification of a material and its attribution to a rheological type but also for fixation of qualitative changes in the behavior of a sample with the growth of the impact force on it, i.e., also for classification. If so, then generally the absolute values of measures are not of high significance, and

Components of the dynamic modulus for PIB at $T = 20°C$, $\omega = 6.28\ s^{-1}$, and $\gamma = 400\%$

Calculation method	G', kPa		G'', kPa	
	G'_M	G'_L	G''_M	G''_L
Mathematical definition (Eq. (6))	17.08	17.69	21.56	25.44
Fourier analysis (Eq. (4))	17.25	17.49	28.03	23.13
Integration (Eqs. (8) and (10))	31.86	17.63	36.77	24.54
Calculation for the first harmonic	17.48		24.27	

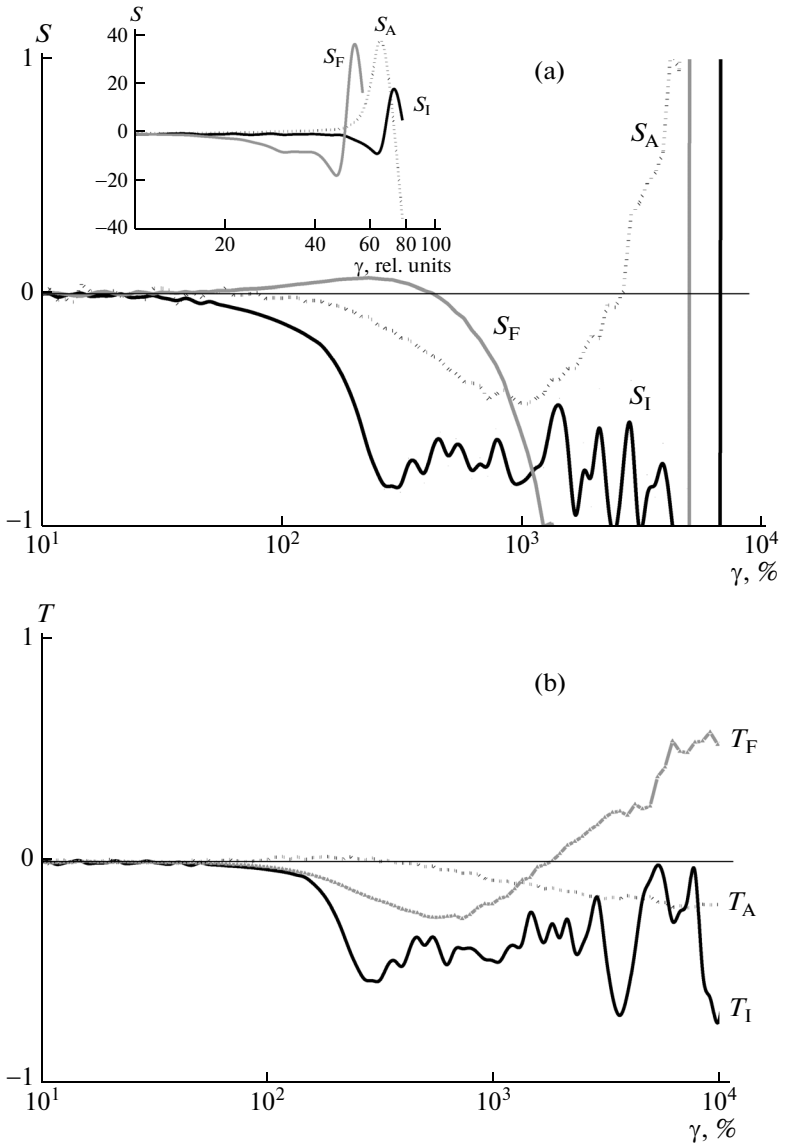

Fig. 4. Measures of (a) elastic and (b) viscous nonlinearity of PIB at 20°C and an angular frequency of 6.28 s^{-1}.

any method convenient for the experimenter is acceptable for classification.

Because all the methods give close values of moduli at the same value of the deformation amplitude, it is reasonable to restrict ourselves to sample classification only for the definition of any single modulus at two different deformation amplitudes. This seems to be possible on the basis of the fact that modulus $G_{M,I}$ is calculated only from the value of modulus $G_{L,I}$ at two different values of the deformation amplitude (Eqs. (9) and (10)). In addition, the nonlinearity measure is the ratio of moduli at high and minimal deformations (Eq. (7)). Then, for estimation of the measures of nonlinearity, i.e., for material classification, it is enough to define two moduli, for example, for the first harmonic. This is topical because the modulus of the first harmonic practically coincides with the integral modulus at a large deformation, $G_{L,I}$ (Fig. 3).

There is a problem consisting in the absence of an independent basis for a judgment about the correctness of nonlinear measures. If, for T as a measure of nonlinearity of viscous properties, it is possible to compare for confirmation its amplitude dependence with the flow curve of the studied sample, then the application of elastic measure S for judgment about correctness is not obvious.

The following question can be posed: Is there any dependence of the measure of nonlinearity on any property of a parameter? It seems that this is the derivative of the property with respect to the mentioned parameter, i.e., the rate of change in the property at an increment in some parameter. If the property is linear,

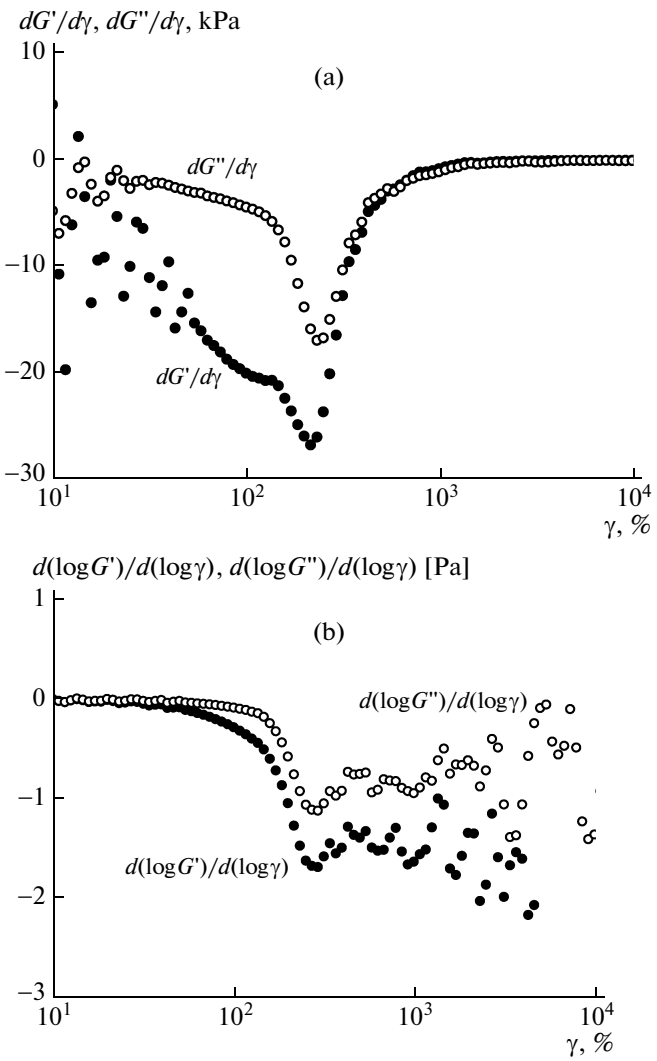

Fig. 5. Amplitude dependences of the derivatives of components of the dynamic modulus with respect to the deformation amplitude for PIB at 20°C and an angular frequency of 6.28 s^{-1}.

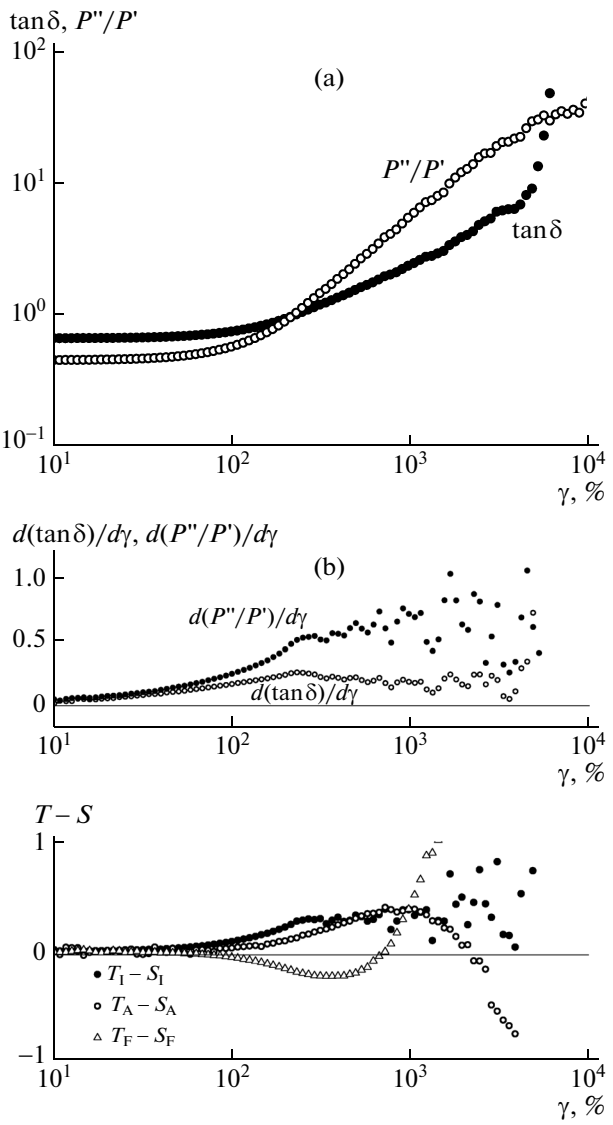

Fig. 6. (a) Amplitude dependences of the mechanical-loss tangent and ratio of the powers of lost and stored energy in the deformation cycle and (b) the correlation of absolute and relative measures of nonlinearity of PIB at 20°C and an angular frequency of 6.28 s^{-1}.

the derivative accepts the zero value. At the same time, the more sensitive the property to the changed parameter, the higher the absolute value of the property derivative. It is apparent that the variable parameter in our case is the deformation amplitude, and the properties are the loss and storage moduli.

The derivatives of the components of the dynamic modulus with respect to the deformation amplitude are presented in Fig. 5a and testify the pseudoplasticity and softening of the sample during shear, an outcome that is generally in good agreement with measures S and T (Fig. 4). Nevertheless, the qualitative resemblance between any curves of two figures is not observed. Moreover, the derivatives of moduli indicate considerable softening of the polymer already at small deformations and imply a seemingly absurd transition to linearity of the object with an increase in impact intensity. The explanation consists in the fact that, in the range of small deformations, the moduli are not high and increments of impact amplitudes are small, a situation that leads to the high derivatives. In the region of very large deformation amplitudes, the situation is opposite, and the derivatives are small in absolute value.

For scaling of the analyzed effects, it is necessary to pass to logarithmic values and to consider the derivatives of modulus logarithms with respect to deformation logarithms (Fig. 5b). After calculation, the observed dynamics of variation of the calculated values with an increase in the impact amplitude becomes more realistic. In addition, the comparison of the

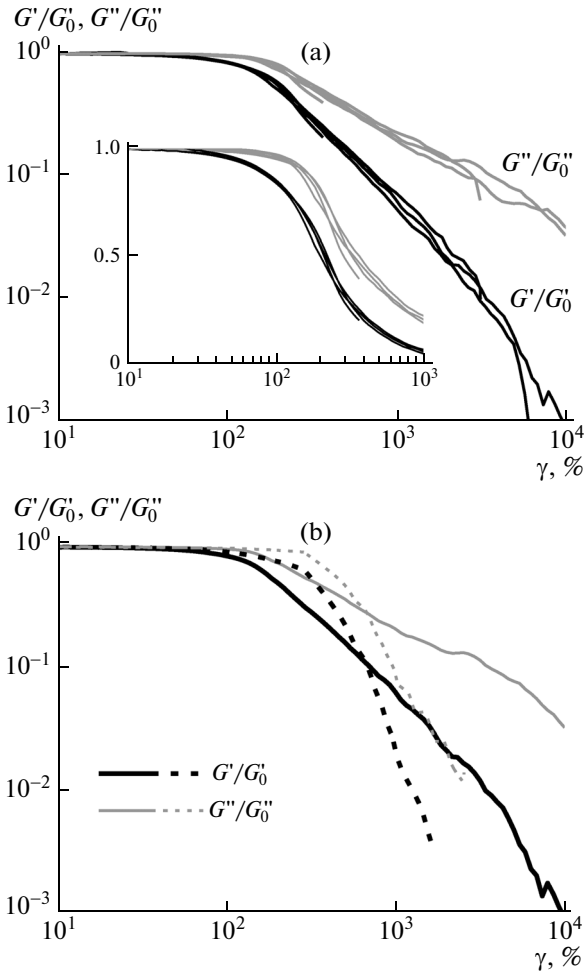

Fig. 7. Amplitude dependences of the normalized moduli of elasticity and loss of PIB (a) at 20°C and frequencies of impact of 1, 3, 10, and 30 Hz and (b) at (solid lines) 20 and (dashed lines) 150°C and a frequency of 3 Hz.

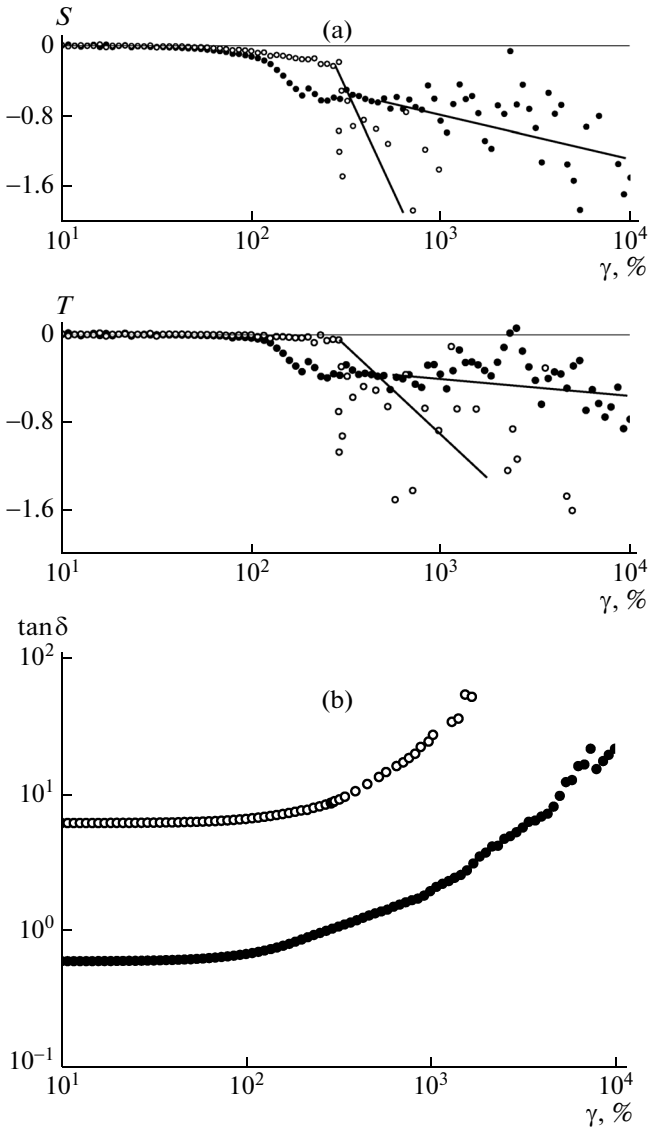

Fig. 8. Amplitude dependences of (a) nonlinearity measures and (b) the mechanical-loss tangent of PIB at (solid circles) 20 and (open circles) 150°C and a frequency of 3 Hz.

derivatives with the measures of nonlinearity found earlier (Fig. 4) indicates the qualitative correlation of the behavior of the derivatives precisely with nonlinearity measures S_I and T_I. This correspondence consists both in the same character of changes in the measures (in their smooth decrease in the region of relatively large deformations and in instability at very large impacts) and in negative values of both parameters as well as in the predominance of the absolute value of an elastic parameter over the viscous parameter.

Discussing the classification of materials from the viewpoint of their softening during deformation, it is appropriate to turn to the classical concept of mechanical-loss angle δ. For its calculation, it is possible to take a pair of the components of the dynamic modulus. Let us use moduli $G'_{L,I}$ and $G''_{L,I}$ as the most convenient ones. Moreover, to define the ratio of lost and stored energy, it is possible to turn to the concept of power of the output signal, which can find separately for stored and lost parts:

$$P' = 0.5\sum_n (G'_n)^2 \quad \text{and} \quad P'' = 0.5\sum_n (G''_n)^2 \qquad (12)$$

The calculations of both parameters testify an increase in the portion of lost energy during sample deformation (Fig. 6a), i.e., its deformation softening. This circumstance is in agreement with the data of Fig. 4, where both nonlinearity measures S and T, regardless of the method of calculation, are mostly negative in the nonlinear region. In addition, S decreases more rapidly with an increase in deformation.

Note that S and T characterize the relative softening of the material during an increase in the impact amplitude from the position of energy storage and loss.

In contrast, tanδ and ratio P''/P' characterize the absolute softening of the material at the given impact amplitude. Consequently, more precise comparison of these two classes of characteristics can be performed in the following manner. First, it is necessary to take the derivative of absolute value (tanδ or P''/P') with respect to deformation in order to transform it into a relative value. Then, the positive value of this derivative will testify the material liquefaction or, in other words, a more intense drop in the value of stored energy with an increase in impact amplitude than that in the lost energy in the same deformation cycle. Because the negative values of relative nonlinearity measures S and T indicate the elastic or viscous softening of the material, the above-mentioned material liquefaction must be observed when the measure of viscous nonlinearity, T, exceeds the magnitude the measure of elastic nonlinearity, S. This means that there must be a qualitative coincidence: If the derivative of tanδ or P''/P' is positive, then the difference between T and S must likewise be positive.

The precise quantitative relationship must proceed from the expression

$$\frac{d\tan\delta}{d\gamma} = \frac{d(G''/G')}{d\gamma} = \frac{G' \times dG''/d\gamma - G'' \times dG'/d\gamma}{(G')^2} = T\frac{\tan\delta}{G''} - S\frac{\tan\delta}{G'} \quad (13)$$

However, for simplicity and clarity, let us restrict ourselves only to a qualitative correlation of the derivatives of absolute values with the difference between the nonlinearity measures calculated previously through three methods (Fig. 4). The data presented in Fig. 6b clearly demonstrate the common character in behavior of the derivatives with the difference of measures S_I and T_I. The differences in two other pairs of measures change their signs with an increase in deformation, whereas the derivatives are positive throughout the considered region of deformation amplitudes.

Hence, the performed analysis revealed that the best result on agreement in behavior with classical characteristics of viscoelasticity are provided by nonlinearity measures S_I and T_I calculated from the moduli found during integration of the Lissajous figures. In this respect, we will use them for further analysis as nonlinearity measures.

Let us establish the character of the effect of the deformation frequency of the material on its nonlinear viscoelasticity. The tests with PIB in the high-elasticity state were performed at a number of angular frequencies (vertical lines in Fig. 1). Figure 7a shows the values of moduli $G'_{L,I}$ and $G''_{L,I}$ normalized to the modulus value in the linear region during sample testing at various frequencies. It is obvious that the normalized moduli of storage and loss take on their characteristic values that are determined by the deformation amplitude, rather than the frequency. The calculation of three different pairs of nonlinearity measures gives precisely the same pattern when the difference between measures S or T at the same deformation, but different frequencies, is dictated only by the test accuracy.

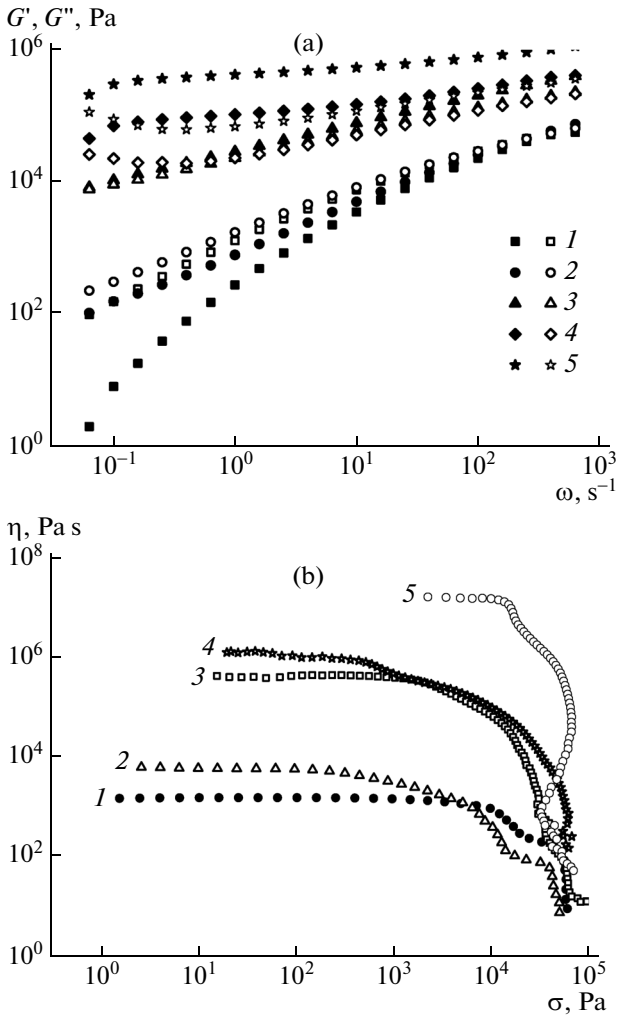

Fig. 9. (a) Frequency dependences of (closed circles) the linear storage and (open circles) loss moduli and (b) flow curves for SiO_2—PIP composites. The volume contents of the filler are (*1*) 0, (*2*) 3, (*3*) 5, (*4*) 7, and (*5*) 9 vol %.

The situation changes qualitatively if we compare the samples in two different relaxation states (Fig. 7b). An increase in temperature and the transition of the polymer from the high-elasticity state to the viscous-flow state cause a broadening of the region of linear viscoelasticity and more drastic decreases in the moduli during output from it with an increase in the impact amplitude. The corresponding behavior is observed for measures of nonlinearity (Fig. 8a), which decrease at 150°C more intensely. It appears that the length of linearity of mechanical properties for the sample in the two relaxation states is, nevertheless, the same, a circumstance that is obvious from the behavior of elastic measure S. Interestingly, the character of the amplitude dependence of the mechanical-loss tangent (as

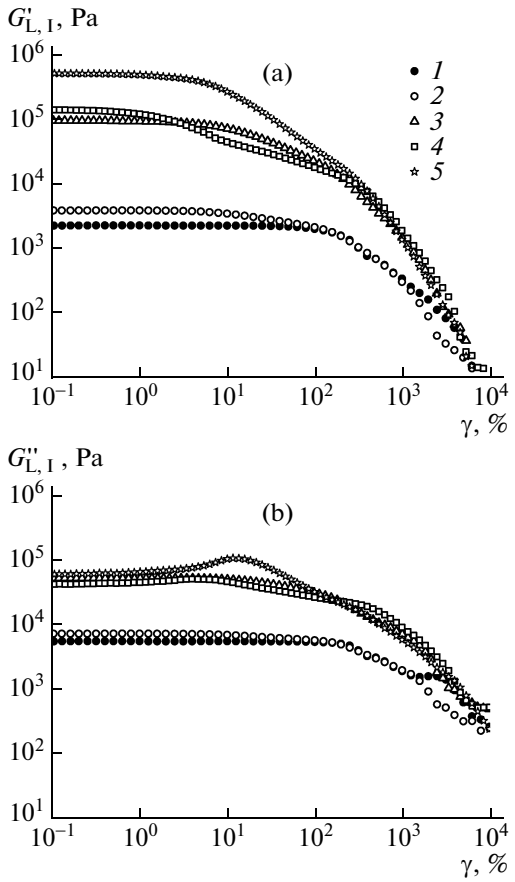

Fig. 10. Amplitude dependences of (a) the storage modulus and (b) the loss modulus for PIP–SiO_2 composites at large deformations. The volume contents of the filler are (*1*) 0, (*2*) 3, (*3*) 5, (*4*) 7, and (*5*) 9 vol %.

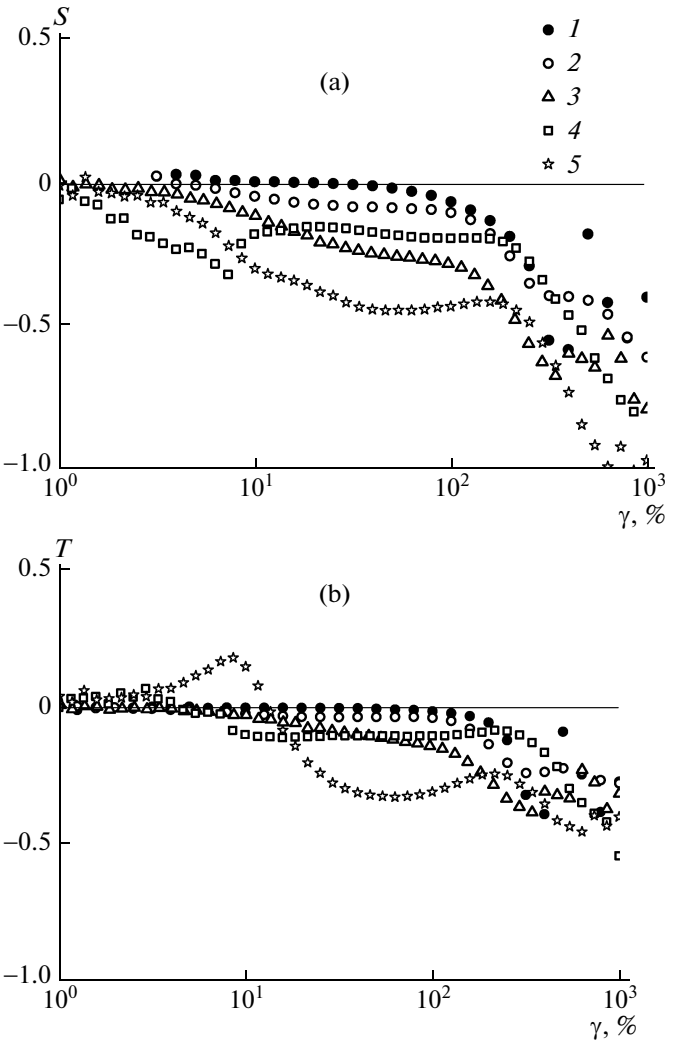

Fig. 11. Amplitude dependences of the (a) elastic and (b) viscous measures of nonlinearity for SiO_2–PIP composites. The volume contents of the filler are (*1*) 0, (*2*) 3, (*3*) 5, (*4*) 7, and (*5*) 9 vol %.

well as the ratio of the powers of lost and stored energy, P''/P') is almost identical for two tests (Fig. 8b), and this occurs during a temperature change of 130°C with a relaxation transition of the sample! Hence, the application of more complex nonlinearity measures for comparison of the objects and analysis of their behavior, instead of that of the conventional mechanical-loss tangent, seems justified.

Polyisoprene Nanocomposite

Let us consider now which new information about the material can be derived from the method of large deformations. Let us take for analysis synthetic rubber filled with nanoparticles, and to start, let us follow the evolution of linear viscoelastic properties and viscosity during an increase in the filler content. The practical interest is due to the application of similar filled elastomers as adhesives [37].

The addition of particles to the polymer leads to increases in both components. In addition, more intense increases are observed in the low-frequency region (Fig. 9a). As a result, at silicon dioxide contents of 7–9 vol %, the storage and loss moduli can be considered values that almost do not depend on frequency. Presumably, the addition of silicon dioxide nanoparticles to PIP favors an increase in the rigidity of the composite due to the formation of fractal spatial chains by the particles with a low affinity for the matrix that are combined into a single network. This situation causes the transition of the material from a viscous-flow relaxation state to a pseudo-rubbery gel state.

The evolution of the flow curves reflects an increase in the degree of sample filling with an increase in viscosity (Fig. 9b). The formation of the spatial network in the sample is not so evident, because, even if the material reaches the yield stress, its value practically coincides with the stress for the polymer transition to a forced high-elasticity state. However, the flow curve of the composite with 9 vol % SiO_2 has an *S* shape with

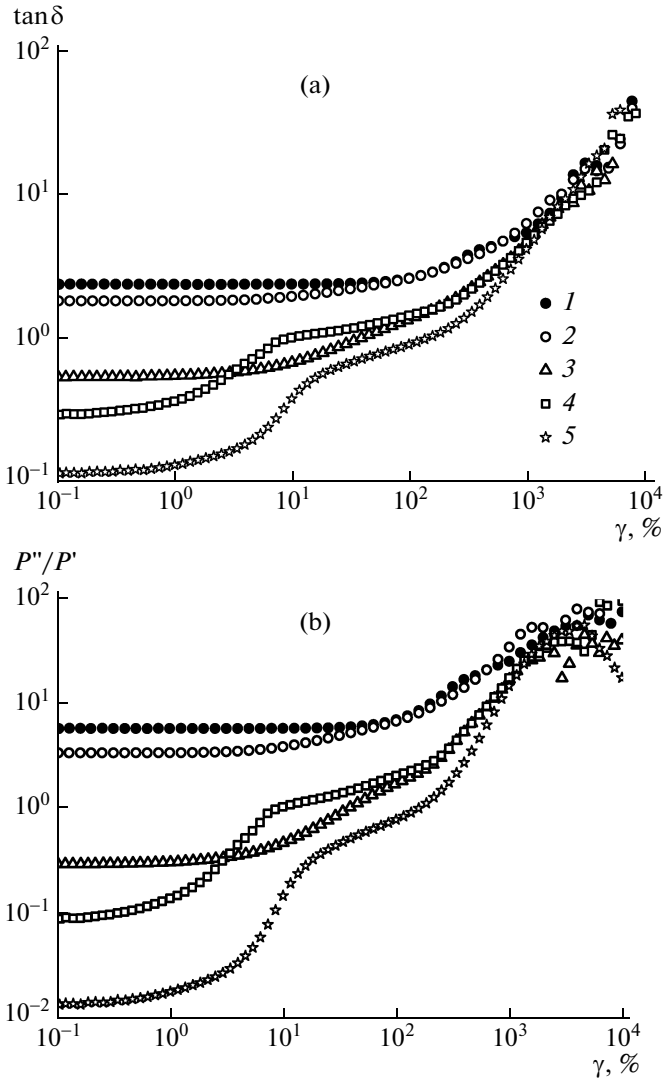

Fig. 12. Amplitude dependences of the (a) the mechanical-loss tangent and (b) ratio of the powers of lost and stored energy for SiO_2—PIP composites. The volume content of the filler are (*1*) 0, (*2*) 3, (*3*) 5, (*4*) 7, and (*5*) 9 vol %.

the differential viscosity becoming negative. Such behavior is characteristic for concentrated suspensions and is connected with decomposition of the spatial network from the particles during passage through the yield stress [38, 39].

Let us consider the evolution of the integral components of the dynamic modulus (Fig. 10). It is apparent that, for the absolute magnitudes of moduli, a series of curves decomposes into two sets. This outcome indicates the transition in the structural state of the material in the range of silicon dioxide contents of 3–5 vol %. Presumably, the matter is the transition via the percolation barrier of nanoparticles that results in the formation of a spatial network in the whole material bulk [40]. Precisely the presence of such a solid network causes the high moduli for more concentrated compositions. The introduction of the particles reduces the length of the region of linear viscoelasticity, a result that is noticeable also for the composition with 3 vol % filler. The latter is likely to imply the presence in the sample of separate aggregates decomposing during the action of shear, even at a particle content below the percolation barrier.

The network formed by the particles in the sample is rigid and starts to decompose at deformation amplitudes of ~1%. Then, as the impact force increases, the viscoelastic properties of the samples approach the values characteristic for the matrix polymer. Interestingly, at a particle content in the composite of 5 vol % or more (especially evident for the sample with 9 vol % SiO_2), the amplitude dependence of the loss modulus starts to pass through the maximum. Hence, as the portion of the filler increases, the transition of the rheological behavior of the material from the archetype with strain thinning to the archetype with a weak strain overshoot occurs [41]. The last archetype is exactly characteristic for suspensions of silicon dioxide particles with the structure that decomposes during shear [42, 43].

Let us consider the evolution of nonlinear measures (Fig. 11). Both measures testify the viscous and elastic softening of the composites during their deformation and the strengthening of nonlinearity with an increase in the filler content. The exception is the system with 9 vol % filler, for which the viscous measure indicates the dilatant behavior at not very large deformations. This effect is likely caused by rheopexy at low deformation rates, as is typical for concentrated suspensions [44].

The absolute measures of material softening in this case are informative (Fig. 12), unlike those applied for consideration of the difference between the polymer in two different relaxation states (Fig. 8b). In this case, the concentration boundary between the character of behavior of the samples shifts to the higher contents of particles, and for systems with contents of silicon dioxide of 7–9 vol %, some deformation transitions are clearly observed, a circumstance that is not characteristic for less filled composites; i.e., the absolute characteristics of softening, although they include both elastic and viscous components, appear to be useful for analysis of the sample properties. In addition, the two sets of curves differ not only in character but also in length of the starting region of linearity in which the softening measures of the sample do not change during an increase in the impact force. Thus, for composites with 7 and 9 vol % filler, the portion of stored energy in the cycle of deformation begins to extremely decrease as early as at low shear amplitudes.

Finally, note the difference between the two absolute characteristics of softening: tanδ and P''/P'. During the application for comparison of the samples of tanδ, the difference between the samples is not as high as during the comparison of the energy characteristics

during their deformation. In other words, the ratio of lost power and stored power as the nonlinearity characteristics during deformation may be preferable for application owing to the higher resolution during differentiation between the compared systems.

Hence, the method of large amplitude oscillatory shear is useful for observations of qualitative structure transitions in samples during variation in their composition and observations of the peculiarities of decomposition of the structures under shear.

CONCLUSIONS

The numerical values of the components of the dynamic modulus at large amplitude oscillatory shear slightly depend on the choice of a particular method for their calculation. In contrast, the sign of the nonlinearity measures of the material, which indicates its type of rheological behavior as well as the character of variation of the numerical parameter of these measures with an increase in the deformation amplitude, is individual for each of the compared methods. The nonlinearity measures may characterize both the absolute change in the ratio of lost energy and stored energy in the sample during its cyclic deformation and the relative changes in the viscous and elastic components as the material moves away from the region of linearity of mechanical properties. The application of different nonlinearity measures can serve for classification and comparison of the behavior of samples at large deformations without application for such analysis of particular rheological models.

ACKNOWLEDGMENTS

I am grateful to A.Ya. Malkin and V.G. Kulichikhin for the discussion of this study.

This work was supported by the Russian Science Foundation, project no. 14-23-00003.

REFERENCES

1. A. Ya. Malkin and A. I. Isayev, *Rheology: Concepts, Methods, and Applications* (ChemTecPubl., Toronto, 2012).
2. R. H. Ewoldt, C. Clasen, A. E. Hosoi, and G. H. McKinley, Soft Matter **3**, 634 (2007).
3. P. Ptaszek, J. Food Eng. **146**, 53 (2015).
4. H. Komatsu, T. Mitsui, and S. Onogi, Trans. Soc. Rheol. **17**, 351 (1973).
5. K. Hyun, M. Wilhelm, C. O. Klein, K. S. Cho, J. G. Nam, K. H. Ahn, S. J. Lee, R. H. Ewoldt, G. H. McKinley, Prog. Polym. Sci. **36**, 1697 (2011).
6. C. Bia, D. Lia, L. Wang, Y. Wang, B. Adhikarid, Carbohydr. Polym. **92**, 1151 (2013).
7. S. Ozkan, T. W. Gillece, L. Senak, and D. J. Moore, Int. J. Cosmet. Sci **34**, 193 (2012).
8. M. Kempf, D. Ahirwal, M. Cziep, and M. Wilhelm, Macromolecules **46**, 4978 (2013).
9. D. Ahirwal, S. Filipe, I. Neuhaus, M. Busch, G. Schlatter, M. Wilhelm, J. Rheol **58**, 635 (2014).
10. R. Shu, W. Sun, T. Wang, C. Wang, X. Liu, Z. Tong, Colloids Surf., A **434**, 220 (2013).
11. X. Qiao and R. A. Weiss, Macromolecules **46**, 2417 (2013).
12. A. K. Gurnon and N. J. Wagner, J. Rheol. **56**, 333 (2012).
13. D. M. Hoyle, D. Auhl, O. G. Harlen, V. C. Barroso, M. Wilhelm, T. C. B. McLeish, J. Rheol. **58**, 969 (2014).
14. J.-E. Bae and K. S. Cho, J. Rheol. **59**, 525 (2015).
15. S. A. Rogers, J. Rheol. **56**, 1129 (2012).
16. J. Kim, D. Merger, M. Wilhelm, and M. E. Helgeson, J. Rheol. **58**, 1359 (2014).
17. S.-Q. Wang, Y. Wang, S. Cheng, X. Li, X. Zhu, H. Sun, Macromolecules **46**, 3147 (2013).
18. R. Salehiyan, Y. Yoo, W. J. Choi, and K. Hyun, Macromolecules **47**, 4066 (2014).
19. M. R. B. Mermet-Guyennet, J. G. de Castro, M. Habibi, N. Martzel, M. M. Denn, D. Bonn, J. Rheol. **59**, 21 (2015).
20. M. Laurati, S. U. Egelhaaf, and G. Petekidis, J. Rheol. **58**, 1395 (2014).
21. C. Perge, N. Taberlet, T. Gibaud, and S. Manneville, J. Rheol. **58**, 1331 (2014).
22. F. Cyriac, J. A. Covas, L. H. G. Hilliou, and I. Vittorias, Rheol. Acta **53**, 817 (2014).
23. J. M. Kim, A. P. R. Eberle, A. K. Gurnon, L. Porcar, N. J. Wagner, J. Rheol. **58**, 1301 (2014).
24. S. O. Ilyin, V. G. Kulichikhin, and A. Y. Malkin, Polym. Sci., Ser. A **55** (8), 503 (2013).
25. R. H. Ewoldt, J. Rheol. **57**, 177 (2013).
26. R. H. Ewoldt and N. A. Bharadwaj, Rheol. Acta **52**, 201 (2013).
27. Z. Fahimi, C. P. Broedersz, T. H. S. van Kempen, D. Florea, G. W. M. Peters, H. M. Wyss, Rheol. Acta **53**, 75 (2014).
28. J. J. Stickel, J. S. Knutsen, and M. W. Liberatore, J. Rheol. **57**, 1569 (2013).
29. J. W. Swan, R. N. Zia, and J. F. Brady, J. Rheol. **58**, 1 (2014).
30. M. Wilhelm, Macromol. Mater. Eng. **287**, 83 (2002).
31. K. S. Cho, K. Hyun, K. H. Ahn, and S. J. Lee, J. Rheol. **49**, 747 (2005).
32. K. Atalik and R. Keunings, J. Non-Newtonian Fluid. Mech. **122** 107 (2004).
33. R. H. Ewoldt, A. E. Hosoi, and G. H. McKinley, J. Rheol. **52**, 1427 (2008).
34. S. Ilyin, V. Kulichikhin, and A. Malkin, Appl. Rheol. **24**, 13653 (2014).
35. S. O. Ilyin, A. Y. Malkin, and V. G. Kulichikhin, Polym. Sci., Ser. A **56** (1), 98 (2014).

36. J. D. Ferry, *Viscoelastic Properties of Polymers* (Wiley, NewYork, 1980).
37. A. Kostyuk, V. Ignatenko, N. Smirnova, T. Brantseva, S. Ilyin, S. Antonov, J. Adhes. Sci. Technol. **29** (17), 1831 (2015).
38. N. B. Uriev, Russ. Chem. Rev. **73**, 37 (2004).
39. A. Y. Malkin, S. O. Ilyin, A. V. Semakov, and V. G. Kulichikhin, Soft Matter **8**, 2607 (2012).
40. S. O. Ilyin, A. Y. Malkin, V. G. Kulichikhin, A. Y. Shaulov, E. V. Stegno, A. A. Berlin, S. A. Patlazhan, Rheol. Acta **53**, 467 (2014).
41. K. Hyun, S. H. Kim, K. H. Ahn, and S. J. Lee, J. Non-Newtonian Fluid. Mech. **107**, 51 (2002).
42. S. R. Raghavan and S. A. Khan, J. Colloid Interface Sci. **185**, 57 (1997).
43. F. Yziquel, P. J. Carreau, and P. A. Tanguy, Rheol. Acta **38**, 14 (1999).
44. N. B. Uriev, Prot. Met. Phys. Chem. Surf. **46**, 1 (2010).

Translated by K. Aleksanyan